Aerodynamics of Very Slender Rectangular Wing Bodies to High Incidence

Erik S. Larson*
Aeronautical Research, Institute of Sweden, FFA, Stockholm, Sweden

Results from slender body theory and linearized theory have been used to formulate semiempirical expressions for steady, symmetric aerodynamic coefficients of a family of slender wing-body combinations up to angles of attack of about 50 deg. The wing planform is restricted to rectangular wings with an exposed aspect ratio of less than 0.5. The results indicate the capability of slender body theory and linearized theory to provide a basis for the construction of short-cut methods, usable in an early stage of project design where flow situations are still too complicated to be handled by more advanced theories. In order to obtain the present result, it has been necessary to make use of subjective assumptions and an empirical correlation. The result, therefore, is not unique. It is, however, a step toward a practical analytic representation of the symmetric aerodynamic characteristics of the family of wing-body combinations treated herein.

Nomenclature

A	= exposed aspect ratio, $(b-D)^2/S$
$A_{1,2}$	= projected partial surfaces of the body
b	= span of wing-body combination
ΔC_D	= lift-dependent drag coefficient = lift dependent drag/qS
C_{d_n}	= cylinder crossflow drag coefficient
C_N	= normal force coefficient = normal force/qS
C_m	= pitching-moment coefficient = pitching moment/qSD
c	= root chord
D	= body diameter, reference length, drag
f, f_1	= correction factors
$g\{R/s\}$	= see Eq. (2)
K_p	$= \partial(C_{Np})\partial(\sin\alpha\cos\alpha)$
$K_{v,\mathrm{le}}$	= ∂(two times leading edge suction force from one side/qS) $/\partial\sin^2\alpha$
$K_{v,\mathrm{se}}$	= ∂(two times tip suction force from one side/qS) $/\partial\sin^2\alpha$
L	= length of the body
L_a	= length of the afterbody
L_n	= nose length
M	= free stream Mach number
N	= normal force
q	= freestream dynamic pressure
R	= radius of the body
S	= reference area, $\pi D^2/4$
s	= half span of wing-body combination
x	= length coordinate, measured streamwise either from body apex or from the wing leading edge
α	= angle of attack
$\bar{\alpha}$	$= \alpha \mp \Delta\alpha$; upper sign for $\alpha \geq 0$, lower sign for $\alpha < 0$
$\Delta\alpha$	$= [0.14(\alpha \mp \alpha_{st})]^2$, $\alpha \geq \alpha_{st}$, empirical correction; signs as for $\bar{\alpha}$
α_{st}	$= 23.5 + (9.2 - c/D)\,[4(1-R/s)^2]^{-1}$, empirical correction
β	$= \sqrt{1-M^2}$
η	= correction factor depending on length of the cylinder
ξ	= dimensionless length coordinate, x/D
ξ_{ref}	= reference point at $0.55L$ from nose of body

Subscripts

B	= body
$B(W)$	= body in presence of wing
W	= wing
$W(B)$	= wing in presence of body
WB	= wing-body combination
ac	= center of pressure
cg	= center of gravity
fb	= forebody
i	= interference
k,ℓ	= different partial contributions
n	= nose
p	= potential or attached flow
pr	= projection
st	= stall
v,le	= vortex effect at the leading edge
v,se	= vortex effect at the side edge

Introduction

IT was recognized quite early by Ward,[1] Flax and Lawrence,[2,3] and Morikawa,[4] that ratios between partial loads on a wing-body combination were practical and flexible tools for short-cut methods usable in early project design work. The well-known coefficients K_W and K_B were derived by slender body theory and were found to be applicable not only to slender configurations but also to configurations with wings of larger aspect ratios; however, restrictions on minimum length of afterbody had to be observed[5] for capturing full interference on the body caused by the wing. The contributions were all obtained in the supersonic speed domain, and the angles of attack were low. It is reasonable to assume, within the concept of slender configurations, that the characteristic ratios would also be applicable at transonic and subsonic speeds. A systematic test of this has not been accomplished yet.

The purpose of this article is to present semiempirical expressions for total aerodynamic coefficients of very slender rectangular wing-body combinations at low speed and up to high incidence. For the derivation experimental results, characteristic ratios and results from linearized theory are used. The analytic expressions are quantified through empirical correlation. Resulting constants, thus, depend on the particular test models and test conditions. Workable analytic expressions of this kind would be flexible tools in preliminary design work. In addition, the result could serve as a complement to other prediction methods which either do not give the very slender rectangular wing a special treatment or ex-

Received May 3, 1983; revision received July 13, 1983.

*Senior Research Engineer, Department of Aerodynamics. Member AIAA.

clude very slender wings from the domain of applicability. An example of the former situation is the high-incidence (from 0 to 180 deg) result obtained by Joergensen,[6] and an example of the latter is the Missile 1 prediction code by Nielsen et al.[7]

Recent low-speed experimental results[8] on very slender wing-body combinations up to angles of attack of 45 deg are well suited for the present construction of semiempirical expressions. The configurations tested in Ref. 8 consisted of a body of revolution with a blunt nose and a set of nine slender rectangular wings in midwing position. Figure 1 shows the configurations with largest and smallest wings, and the inserted table provides the parameters for the test models. The wing span and root chord are varied so that the exposed wing aspect ratio is in the interval $0.1<A<0.3$. The total body length is held constant.

The presently derived semiempirical result is restricted to subsonic speed, and to steady and symmetric total coefficients.

Semiempirical Modeling

Normal Force Coefficient

The normal force on a slender wing-body configuration is composed of partial loads that are combined as

$$N_{WB}=N_B+(N_W+N_{Wi})\left(1+\frac{N_{Bi}}{N_W+N_{Wi}}\right) \tag{1}$$

in order to make use of a result from slender body theory obtained by Lawrence and Flax,[3] namely

$$\frac{N_{Bi}}{N_W+N_{Wi}}=\frac{R}{s}\,\frac{(1-R/s)+1/3[1-(R/s)^3]}{1-(R/s)^2}=g\{R/s\} \tag{2}$$

Equation (2) is the ratio between the normal force on the body caused by interference from the wing and the total normal force on the wing in situ. It is assumed that Eq. (2) holds, irrespective of the nose shape and the forebody length; i.e., irrespective of the downwash from the forebody vortices. The denominator in Eq. (2) is approximated by

$$N_W+N_{Wi}=N_{W(B)}=N_W(1+N_{Wi}/N_W)$$
$$=N_W(1+R/s+f_l) \tag{3}$$

The term R/s is the Beskin upflow result,[9] and f_l is an empirical correction factor.

The normal force on the rectangular wing alone is obtained by linearized theory (extended Multhopp method) according to Lamar[10] and the suction force analogy by Polhamus.[11] The total normal force coefficient, referred to the body cross section, for the wing in the presence of the body is

$$C_{N_{W(B)}}=4/\pi(c/D)\ (s/R-1)\ (1+R/s+f_l)$$
$$\times[K_p\sin\alpha\ \ \cos\alpha+\ (K_{v,\mathrm{le}}+K_{v,\mathrm{se}})\sin^2\alpha] \tag{4}$$

The K coefficients have been determined numerically by Lamar,[10] and are represented by semiempirical expressions[12] compiled in the Appendix. For the small aspect ratios of interest here ($A<0.5$), K_p, and K_v,le can be approximated by straight lines, as shown in Fig. 2, where $K_{v,se}$ is plotted also for comparison with Lamar's[10] result.

The normal force on the body, N_B in Eq. (1), refers to the gross body except for the length covered by the root chord c. The normal force coefficient for this reduced body is obtained by results from slender body theory developed by Munk,[13] Allen and Perkins,[14] and Kelly,[15] and compiled by Joergensen,[16] and are

$$C_{N_B}=\sin 2\alpha\cos(\alpha/2)+\eta C_{d_n}\ (A_{pr}/s)\ \sin^2\alpha \tag{5}$$

where $A_{pr}=A_l+A_2$ is the sum of the projected areas of the fore- and afterbody.

A preliminary evaluation of Eqs. (1-5) shows that a correction factor f_l is needed for decreasing c/D (i.e., for increasing afterbody lengths), and that at the higher angles of attack, a correction $\Delta\alpha$ due to start of stall improves the correlation with experiment.[8] Furthermore, it seems practical to use an explicit correction term instead of connecting it to the upwash term as in Eq. (4).

Compiling the above results for the normal force coefficient on wing-body combinations of the type discussed here, results in the following semiempirical expressions:

$$C_{N_{\mathrm{WB}}}=\sin 2\alpha\cos(\alpha/2)+\eta C_{d_n}(A_{pr}/s)\ \sin^2\alpha$$
$$+\frac{4}{\pi}(c/2s)\ [(s/R)^2-1]\ [K_p\sin\bar{\alpha}\cos\bar{\alpha}$$
$$+(K_{v,\mathrm{le}}+K_{v,\mathrm{se}})\ \sin^2\bar{\alpha}](1+g\{R/s\})$$
$$\times(1+f\{R/s,\ c/D\}) \tag{6}$$

where $\bar{\alpha}$ contains empirical corrections, $\Delta\alpha$ and α_{sl} (see Nomenclature), for the effects caused by start of stalling and vortex breakdown. The corrections are constructed by means of the test results in Ref. 8 (nine configurations). Other relevant results for a control of $\Delta\alpha$ and α_{sl} in the low-speed domain have not been found in the literature. The correction

b/D	c/D	A	L_a/D	b/D	c/D	A	L_a/D	b/D	c/D	A	L_a/D
2.43	7.32	0.20	3.68	2.15	7.32	0.15	3.68	1.48	4.83	0.10	6.17
	5.93	0.25	5.07		5.93	0.20	5.07		3.24	0.15	7.76
	4.95	0.30	6.05		4.76	0.25	6.24		2.44	0.20	8.56

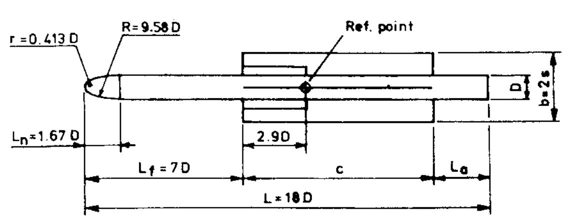

Fig. 1 The wind tunnel test models of Ref. 8. Largest and smallest wing attached to the body are shown with a table of geometric parameters of all nine wings.

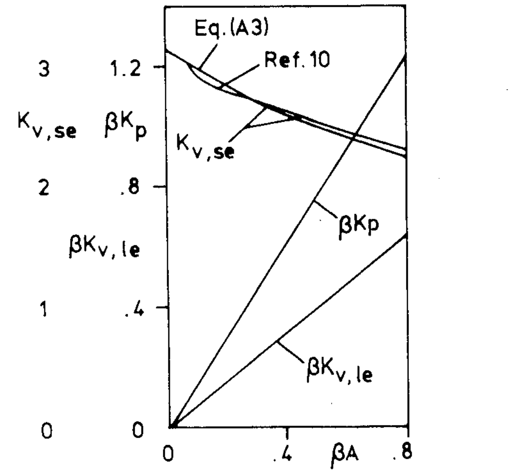

Fig. 2 *K* coefficients for small aspect ratio rectangular wings.

factor f is taken to be

$$f\{R/s,c/D\} = \frac{9}{4}\left(\frac{R/s-2/9}{R/s+1}\right)\left(\frac{19/4-c/D}{19/4+c/D}\right)$$

$$R/s \geq 2/9, \quad c/D \leq 19/4 \tag{7}$$

The K coefficients for $A<0.5$ are given in the Appendix [Eqs, (A3-A5)] and the factor $g\{R/s\}$ is given by Eq. (2). It may be noted that for $\bar{\alpha}<0$ the factor $\sin^2\bar{\alpha}$ must be treated as $|\sin\bar{\alpha}|\sin\bar{\alpha}$.

The corrections introduced here are derived under the restriction that the sum of chord and afterbody is a constant, namely,

$$c+L_a = \text{const} = 11D \qquad c,L_a \neq 0 \tag{8}$$

which characterizes the test models of Ref. 8 (Fig. 1).

The Lift-Dependent Drag Coefficient

The lift-dependent drag coefficient of the wing-body combination is obtained by

$$\Delta C_{D_{\mathrm{WB}}} = C_{L_{\mathrm{WB}}} \cdot \tan\alpha = C_{N_{\mathrm{WB}}} \cdot \sin\alpha \tag{9}$$

A comparison with experiment is not possible because such data are not available.

The Pitching-Moment Coefficient

The pitching-moment coefficient on the wing-body combination is first written in a general form as

$$C_{m_{\mathrm{WB}}} = \sum^{k} C_{N_B}(k)\cdot\Delta\xi_B(k) + \sum^{\ell} C_{N_W}(\ell)\cdot\Delta\xi_W(\ell) + C_{N_{B(W)}}\cdot\Delta\xi_{B(W)} + C_{m_{0B(W)}} \tag{10}$$

where

$$\Delta\xi_B(k) = \xi_{\mathrm{ref}} - \xi_{\mathrm{cg}}(k) \tag{11}$$

for the body, and

$$\Delta\xi_W(\ell) = \xi_{\mathrm{ref}} - \xi_{\mathrm{le}} - \xi_{ac}(\ell) \tag{12}$$

for the wing. According to Eq. (6) $k=\ell=3$; ξ_{ac} is counted from the leading edge of the wing; $\xi_{\mathrm{ref}}=9.9$ (i.e., 55% of the body length); and $\xi_{\mathrm{le}}=7$. These parameters are constant for all of the configurations investigated.

The last term in Eq. (10) could represent a moment originating from the interference on the body, but it is neglected here because of lack of relevant data. The different partial normal force contributions are given in Eq. (6). Simple expressions will be assumed for the respective distances between the reference point and the different centers of pressure. Equations (10-12) written in more detail are

$$\begin{aligned} C_{m\mathrm{WB}} &= \sin 2\alpha\cos(\alpha/2)\cdot\Delta\xi_{Bp} + \eta C_{d_n} \\ &\times\left(\frac{A_1}{S}\cdot\Delta\xi_{BA_1} + \frac{A_2}{S}\cdot\Delta\xi_{BA_2}\right)\sin^2\alpha \\ &+ \frac{4}{\pi}(c/2s)\left[(s/R)^2-1\right]\left[K_p\sin\bar{\alpha}\cos\bar{\alpha}\cdot\Delta\xi_{Wp}\right. \\ &+ \left.(K_{v,\mathrm{le}}\cdot\Delta\xi_{W_{v,\mathrm{le}}} + K_{v,\mathrm{se}}\cdot\Delta\xi_{W_{v,\mathrm{se}}})\sin^2\bar{\alpha}\right] \\ &\times(1+f\{R/s,\,c/D\}) + C_{N_{W(B)}}\cdot g\{R/s\}\cdot\Delta\xi_{B(W)} \end{aligned} \tag{13}$$

where $C_{N_{W(B)}}$ is equivalent to the third term in Eq. (6), reduced by the factor $[1+g(R/s)]$, and

$$\Delta\xi_{Bp} = \xi_{\mathrm{ref}} - \epsilon_{\mathrm{cg}_B} = (8.79) \tag{14a}$$

if the empirical correction factors f and $\Delta\alpha$ could be derived directly from the actual flow situation, experimentally or theoretically.

$$\Delta\xi_{A1} = \xi_{\mathrm{ref}} - \epsilon_{\mathrm{cg}_{A1}} = (6.23) \tag{14b}$$

$$\Delta\xi_{A2} = \xi_{\mathrm{ref}} - \epsilon_{\mathrm{cg}_{A2}} = -2.6\text{-}0.5\,L_a/D \tag{14c}$$

for the body, and

$$\Delta\epsilon_{w_p} = \xi_{\mathrm{ref}} - \xi_{\mathrm{le}} - (c/4D)A(1+A^2)^{-1/2} \tag{15a}$$

$$\Delta\epsilon_{w_{v,\mathrm{le}}} = (\xi_{\mathrm{ref}} - \xi_{\mathrm{le}})\cos\alpha = (2.9)\cos\alpha \tag{15b}$$

$$\Delta\epsilon_{w_{v,\mathrm{se}}} = \xi_{\mathrm{ref}} - \xi_{\mathrm{le}} - (c/2D)\cos(\alpha/2) \tag{15c}$$

$$\Delta\xi_{B(W)} = \xi_{\mathrm{ref}} - \xi_{\mathrm{le}} - (c/4D) \tag{15d}$$

for the wing. The constant values for the test models of Ref. 8 are given in parentheses. L_a/D in Eq. (14c) is shown in Fig. 1.

Comparison with Experiment

The semiempirical expressions, Eqs. (6-8), which give the normal force coefficient for wing-body combinations of the special type shown in Fig. 1, are evaluated and compared with experiment[8] in Fig. 3. The cruciform wing-body combinations were tested at zero roll angle at $M=0.44$. The Reynolds number was $Re_D=0.8\times10^6$. Evidently the semiempirical representation of the experiment gives a slight overprediction, but, taken as a whole, is quite satisfactory for practical applications. Consequently, it is reasonable to presume that it would be satisfactory for all variants of this type of configuration provided that the exposed aspect ratio of the wing is less than about $A=0.5$.

In Ref. 8, the configuration with the largest wing (Fig. 1) also was tested in a water tunnel ($M_\infty\to0, Re_D=1.25\times10^6$). The normal force data are inserted in Fig. 3a and compared with Eqs. (6-8). The computed result is practically the same as for $M=0.44$ (solid curve). Up to $\alpha=15\text{-}18$ deg the difference between Eqs. (6-8) and the two test results is minor. Above $\alpha=20$ deg the hydrotest result falls below the test result at $M=0.44$; i.e., it is overestimated by Eqs. (6-8). (The pitching-moment data was not reported.)

Improvements of the semiempirical expressions for the normal force are desirable. The best result would be obtained

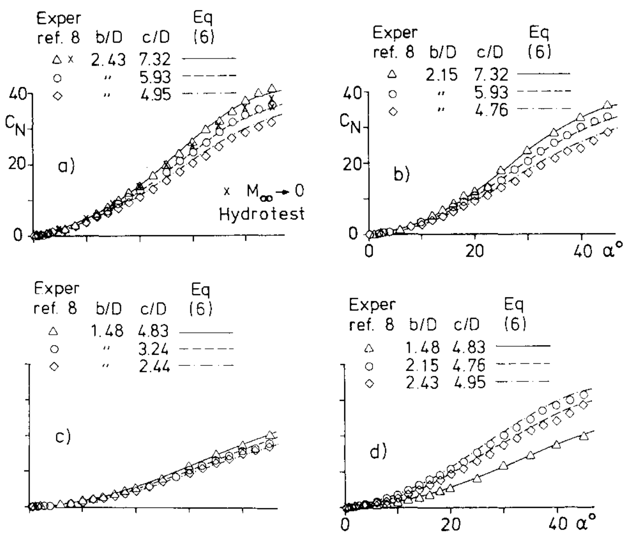

Fig. 3 Total normal force coefficient in incompressible flow ($M=0.44$, $Re_D=0.8\times10^6$) on the wing-body configurations of Fig. 1; a) to c) variation of chord at constant span, and d) variation of span at nearly constant chord.

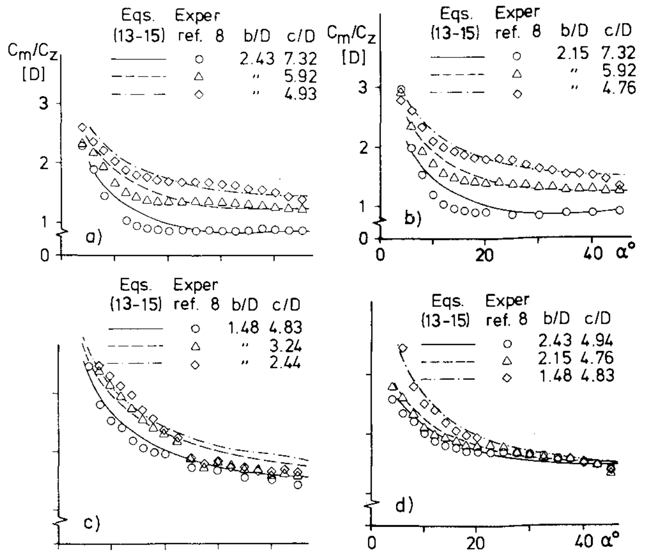

Fig. 4 Center of pressure in incompressible flow ($M=0.44$, $Re_D=0.8\times10^6$) on wing-body configurations according to Fig. 1; a) to c) variation of chord at constant span, and d) variation of span at nearly constant chord.

Equations (13-15), representing the pitching-moment coefficient, are divided by the normal force coefficient, Eq. (6), in order to obtain the location of the center of pressure. The result, expressed in body diameters D, is inserted in Fig. 4 for comparison with experiment.[8] It can be seen that the correlation is not too bad. The discrepancies vary with angle of attack and the largest deviations are found in the interval $10<\alpha<20$ deg for the combinations with the largest span ratios ($s/R=2.43$ and 2.15). It also can be seen that the discrepancy increases when the chord-to-diameter ratio, c/D, decreases, which, in the present context, means an increase of the afterbody length, L_a/D. When the angle of attack is above about 20 deg the difference between the semiempirical representation and experiment decreases. Over the entire angle-of-attack interval, $|\alpha|\leq45$ deg, the discrepancy is less than $D/3$; a result that is quite satisfactory for most practical applications.

A further improvement in the determination of the centers of pressure of the partial loads is desirable. The primary concern is the center of pressure of the interference on the body when the chord is decreased while the length of the afterbody remains constant. This can be obtained by panel methods for the linear part of the interference. For the nonlinear part, partial load measurements or, preferably, pressure measurements on the body are needed, until a theoretical solution is accomplished, perhaps by use of the Euler equations.

Conclusions

The present study demonstrates that slender body theory and linearized theory provide qualitative guidance in formulating semiempirical representations of total coefficients on slender combinations, even in cases where the flow situation is very complicated, and, at present, not manageable by more advanced theories. The result is not unique since it depends on subjective assumptions and an empirical correlation. It is, however, a good first step toward an analytic description of the symmetric characteristics of the configuration family treated herein.

The semiempirical expressions should be applicable throughout the whole subsonic speed domain; however, controlled experiments still remain to be done. The correction factors and the assumed centers of pressure for the partial loads can be improved by experiment and, sooner or later, by numerical solutions of higher order theories.

Appendix

The K coefficients in Eq. (4) are represented by semiempirical expressions in Ref. 12. They are

$$\beta K_p=\frac{2\pi\beta A}{2+\sqrt{(4/3)(\beta A)^2+4}} \tag{A1}$$

$$\beta K_{v,\mathrm{le}}=\frac{\pi\beta A}{2+\sqrt{(1/4)(\beta A)^2+4}} \tag{A2}$$

$$K_{v,\mathrm{se}}=\frac{2\pi}{2+\beta A} \tag{A3}$$

In the case of small aspect ratios ($A<0.5$) investigated here, Eqs. (A1) and (A2) can be simplified to

$$K_p=\frac{\pi}{2}A \tag{A4}$$

$$K_{v,\mathrm{le}}=\frac{\pi}{4}A \tag{A5}$$

and thus are independent of the Mach number. Equation (A4) is recognized as Jones' slender wing result.

Acknowledgment

This work has been supported by the Materiel Administration of the Armed Forces, Air Materiel Department, Missiles Directorate, Sweden.

References

[1] Ward, G. N., "Supersonic Flow Past Slender Pointed Bodies," *The Quarterly Journal of Mechanics and Applied Mathematics,* Vol. II, Pt. 1, No. 3, 1949, pp. 75-97.

[2] Flax, A. H., and Lawrence, H. R., "The Aerodynamics of Low-Aspect Ratio Wings and Wing-Body Combinations," Cornell Aeronautical Laboratory, Rept. CAL-37, Sept. 1951.

[3] Lawrence, H. R., and Flax, A. H., "Wing-Body Interference at Subsonic and Supersonic Speeds. Survey and New Developments," *Journal of the Aeronautical Sciences,* Vol. 21, No. 5, May 1954, pp. 289-324, 328.

[4] Morikawa, G., "Supersonic Wing-Body Lift," *Journal of the Aeronautical Sciences,* Vol. 18, No. 4 April 1951, pp. 217-228.

[5] Nielsen, J. N., *Missile Aerodynamics,* McGraw-Hill Book Co., Inc., New York, 1960.

[6] Joergensen, L. H., "Prediction of Static Aerodynamic Characteristics for Slender Bodies Alone and with Lifting Surfaces to Very High Angles of Attack," NASA TR R-474, Sept. 1977.

[7] Nielsen, J. N., Hemsch, M. J., and Smith, C. A., "A Preliminary Method for Calculating the Aerodynamic Characteristics of Cruciform Missiles to High Angles of Attack Including Effects of Roll Angle and Control Deflections," Rept. ONR-CR215-226-4F, Nov. 1977.

[8] Mifsud, L., "Charactéristiques Aérodynamiques des corps de révolution munis d'ailes d'allongements divers," AGARD Paper 247, 1978.

[9] Kirkby, S., and Robinson, A., "Wing-Body Interference at Supersonic Speeds," College of Aeronautics, Cranfield, Rept. 7, April 1947.

[10] Lamar, J. E., "Extension of Leading-Edge Suction Analogy to wings with Separated Flow around the Side Edges at Subsonic Speeds," NASA TR R-428, Oct. 1974.

[11] Polhamus, E. C., "A Concept of the Vortex Lift of Sharp-Edge Delta Wings Based on a Leading-Edge-Suction Analogy," NASA TN D-3767, Dec. 1966.

[12] Larson, E. S., "Symmetric Flow Characteristics of Thin Rectangular Wings," *Journal of Aircraft,* Vol. 18, Dec. 1981, pp. 1070-1071.

[13] Munk, M. M., "The Aerodynamic Forces on Airship Hulls," NACA Rept. 184, 1923.

[14] Allen, H. J. and Perkins, E. W., "A Study of Effects of Viscosity on Flow over Slender Inclined Bodies of Revolution," NACA Rept. 1048, 1951.

[15] Kelly, H. R., "The Estimation of Normal Foce, Drag and Pitching-Moment Coefficients for Blunt Based Bodies of Revolution at Large Angles of Attack," *Journal of the Aeronautical Sciences,* Vol. 21, No. 8, Aug. 1954, pp. 549-555.

[16] Joergensen, L. H., "Prediction for Static Aerodynamic Characteristics for Space-Shuttle-Like and Other Bodies at Angles of Attack from 0 to 180°," NASA TN D-6996, Jan. 1973.